

## Quantum and classical echoes in scattering systems described by simple Smale horseshoes

C. JUNG<sup>1</sup>, C. MEJIA-MONASTERIO<sup>1</sup> and T.H. SELIGMAN<sup>1,2</sup>

<sup>1</sup> *Centro de Ciencias Físicas, University of Mexico (UNAM), Cuernavaca, Mexico*

<sup>2</sup> *Centro internacional de Ciencias, Cuernavaca, Mexico*

PACS. 05.45.Mt – Semiclassical chaos (“quantum chaos”).

PACS. 03.65.Nk – Scattering theory.

**Abstract.** – We explore the quantum scattering of systems classically described by binary and other low order Smale horseshoes, in a stage of development where the stable island associated with the inner periodic orbit is large, but chaos around this island is well developed. For short incoming pulses we find periodic echoes modulating an exponential decay over many periods. The period is directly related to the development stage of the horseshoe. We exemplify our studies with a one-dimensional system periodically kicked in time and we mention possible experiments.

In classical mechanics the Smale horseshoe [1] construction has proven to be the key point to the understanding of chaotic scattering in time independent systems with two degrees of freedom and time dependent ones with one degree of freedom [2,3]. Though the importance of this construction in the quantum analogue of such systems has been noticed occasionally [4], a study of the implications in quantum systems has not yet been undertaken. We are interested in low-order (such as binary or ternary) horseshoes, where the features encountered are comparatively simple. In the present paper we shall concentrate on situations in which the stage of development of the horseshoe is fairly low. We will discuss a binary horseshoe for which one of the fundamental periodic orbits is hyperbolic and shows homoclinic connections, while the other one is still elliptic and confined inside a large stable island. In such a situation tunneling into the island will be the most notable quantum effect. We shall show that a short pulse as incoming wave leads to periodic pulses in the outgoing wave. They survive many periods and we shall call them echoes. If we use good energy resolution instead we find narrow resonances.

We will focus our discussion on a one-dimensional kicked scattering model mainly because of the ease of calculation, but experiments with similar periodically driven models may be of interest [5]. Yet the effect is not confined to such models. Two-dimensional time-independent billiards with two openings or leads can produce ternary horseshoes with a large central island, whose echoes may be seen in microwave experiments [6] or mesoscopic systems.

The model we use is given in terms of the Hamiltonian

$$H(q, p, t) = \frac{p^2}{2} + A V(q) \sum_{n=-\infty}^{\infty} \delta(t - n). \quad (1)$$

The time dependence is an infinite periodic train of delta pulses kicking the potential with period 1. The parameter  $A$  determines the strength of the potential, which is given by

$$V(q) = \begin{cases} \frac{q^2}{2} + 1 & , \quad q < 0 \\ e^{-q}(q^2 + q + 1) & , \quad q \geq 0 \end{cases} . \quad (2)$$

Note that in the literature [3,7] a similar but simpler potential is used, where the exponential form extends to negative values of  $q$ . We have changed the form of the potential to obtain better convergence of the quantum calculation. Yet the classical results for the two potentials are quite similar. We obtain a smooth development of the binary horseshoe as a function of the parameter  $A$ . The only difference is that for the present potential the development is not entirely monotonic [8], but this does not affect our considerations.

We represent the classical dynamics by a Poincaré map which we choose as the stroboscopic map taken at times  $t = n + 1/2$

$$\begin{aligned} p_{n+1} &= p_n - AV'(q_n + p_n/2) \\ q_{n+1} &= q_n + p_n - AV'(q_n + p_n/2)/2 . \end{aligned} \quad (3)$$

It gives us the evolution of a classical trajectory from time  $n + 1/2$  to time  $n + 3/2$ .

The kicked potential has a maximum at  $q = 1$  and a minimum at  $q = 0$ . It is quite obvious that the points  $p = 0, q = 0$  and  $q = 1, p = 0$  are fixed points of this map. Indeed they represent the fundamental periodic orbits, that determine the construction of the binary horseshoe, which describes the topology of the Hamiltonian flow of our system. The fixed point at  $q = 1$  is obviously hyperbolic, while the other one can vary according to the strength parameter  $A$ . For  $A < 4$  this point is elliptic. At this value it turns inverse hyperbolic, but many secondary islands of stability survive. The phase portrait is hyperbolic when the horseshoe becomes complete near  $A = 6.25$ . Hyperbolic stages are also possible for smaller values of  $A$  for which the horseshoe is incomplete [3,9,10].

We shall focus our attention on the low development stages long before the original elliptic orbit bifurcates. On the other hand we wish to see a well developed chaotic region. These conditions are met for values of  $A$  between 0.5 and 3. We shall use the parameter  $A = 0.967$ . A phase portrait of the stroboscopic map for this value is shown in Fig. 1. This value of  $A$  was chosen because somewhere between this value and  $A = 1$ , the outermost KAM surface shown in Fig. 1 disintegrates.

We are interested in learning about the quantum properties of such a low order horseshoe with a large stable island. For this purpose we use the unitary time evolution operator, which is rather easily obtained for kicked systems. This is the case because the stroboscopic map eq. (3) can be decomposed into three transformations as follows:

$$\begin{aligned} p_{n'} &= p_n \\ q_{n'} &= q_n + p_n/2 \end{aligned} \quad (4)$$

$$\begin{aligned} p_{n''} &= p_{n'} - AV'(q_{n'}) \\ q_{n''} &= q_{n'} \end{aligned} \quad (5)$$

$$\begin{aligned} p_{n+1} &= p_{n''} \\ q_{n+1} &= q_{n''} + p_{n''}/2 . \end{aligned} \quad (6)$$

The second step (5), can be interpreted as a gauge transformation in coordinate space and the other two (4, 6), as a gauge transformations in momentum space. This implies, that

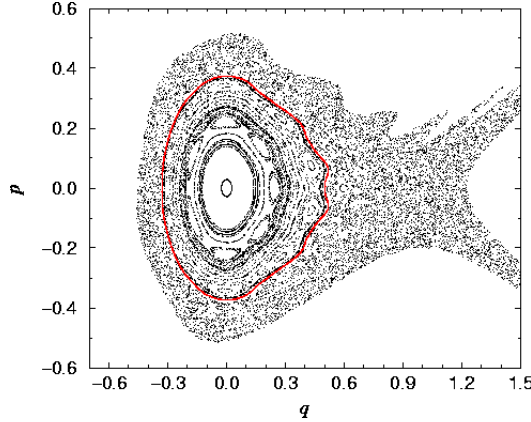


Fig. 1 – Phase portrait of the stroboscopic map eq. (3), for  $A = 0.967$ . Together with the bounded orbits, trajectories corresponding to asymptotic incoming initial conditions are plotted as well. The thick red line corresponds to the outermost KAM surface.

the unitary operator for one time step can be written as three phases intertwined by Fourier transforms  $\mathcal{F}$ , which take us from coordinate to momentum space and back. Thus we obtain for the kernel of this operator in momentum-space

$$U(p', p) = \exp \left[ -\frac{i}{4\hbar} p^2 \right] \mathcal{F} \exp \left[ \frac{i}{\hbar} AV(q) \right] \mathcal{F}^{-1} \exp \left[ -\frac{i}{4\hbar} p^2 \right]. \quad (7)$$

This expression is simple as it involves only Fourier transforms and multiplication with phases. It is also very efficient if good fast Fourier transform (FFT) codes are used.

We shall analyze our scattering system in terms of wave packet dynamics. In all our simulations we use minimum uncertainty Gaussian wave packets given by

$$\Psi(q, 0) = \frac{1}{\pi^{1/4} \sigma^{1/2}} \exp \left[ -\frac{(q - q_{\text{in}})^2}{2\sigma^2} + \frac{i}{\hbar} p_{\text{in}} q \right]. \quad (8)$$

For a given value of the initial momentum  $p_{\text{in}}$ ,  $\sigma$  will determine the duration of the pulse and the value of  $\hbar$  will determine how near to the classical limit we operate. Recall that short pulses imply a poor energy resolution, while long ones can have very well defined energies. We can therefore use short pulses and consider the time evolution in configuration space or in phase space, or we can use long pulses and look at the energy dependence of some outgoing quantity. We shall start with the former and then consider the latter.

First we show in Fig. 2 the Husimi distributions as a function of time superposed to the phase portrait shown in Fig. 1; the Husimi function is indicated by a colour-scale code. We choose the strength parameter  $A = 0.967$  and the wave packet with  $\sigma = 2.5$ ,  $\hbar = 0.01$  and  $(q_{\text{in}} = 100, p_{\text{in}} = -1.48)$ . At time  $t = 68$ , the packet reaches the interaction region, Fig. 2-a. For  $t = 73$ , Fig. 2-b, the packet has entered the potential well near the external fixed point; part of the packet bounces of the barrier and never enters the well. In Fig.2-c, the probability that enters the potential well performs its evolution along the chaotic layer of the phase portrait at  $t = 78$ . For  $t = 86$  most of the packet has left the well. The small remaining probability gets trapped in the potential well where it has tunneled through the surface to inner stable regions, Fig. 2-d. It is interesting to note that for  $A = 1$ , when the KAM-torus has become a classically penetrable cantorus the quantum picture remains unchanged

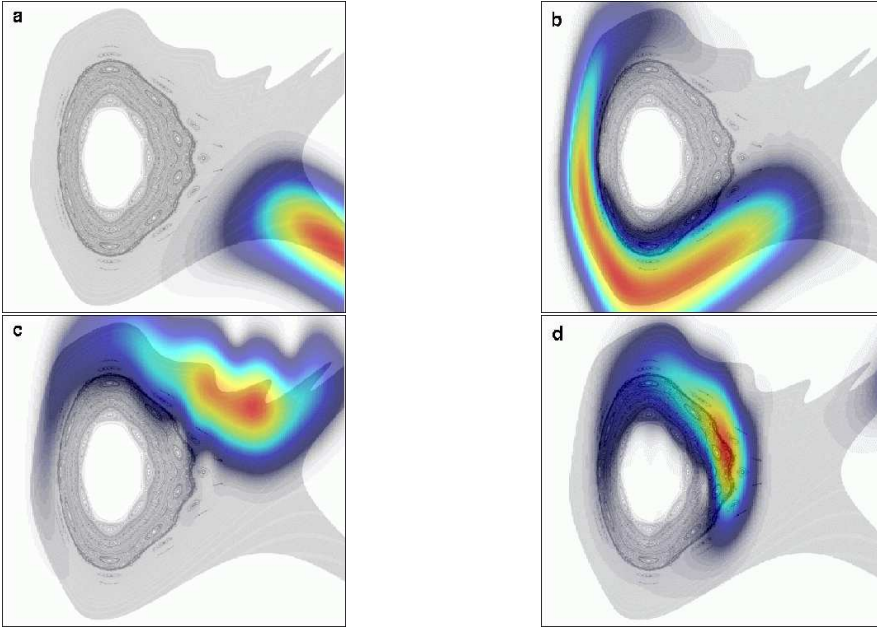


Fig. 2 – Husimi distribution for a wave packet with  $(q_{\text{in}} = 100, p_{\text{in}} = -1.48)$ ,  $\sigma = 2.5$ ,  $\hbar = 0.01$  and  $A = 0.967$  for different times. (a)  $t = 68$ . (b)  $t = 73$ . (c)  $t = 78$ . (d)  $t = 86$ . In these plots, the colour-intensity is different; in particular, (d) exaggerates the intensity.

as diffusion is much slower than tunneling. For larger values of  $A$ , the Husimi distribution will move inwards to be again enclosed by the outermost KAM surface.

Next we show in Fig. 3 the probability distribution in configuration space as a function of time in a logarithmic colour-scale code. The parameters and initial conditions are as above. We clearly distinguish the incoming pulse, the part directly scattered at the barrier and another part that entered the well, but leave directly. This direct scattering corresponds to the one shown in Fig. 2. At longer times we see an oscillating packet inside the well with an amplitude that corresponds to the classically forbidden region in phase space, as shown in Fig. 1. Each time the wave packet returns to the front side (*i.e.* the largest value of  $q$ ) of the well it sends an “echo” to infinity. The time intervals between these echoes corresponds to the oscillation times of the packet inside the stable island which in turn corresponds to the average classical winding time of the invariant surfaces in the region of phase space where the packet oscillates. Note that the winding time near the surface of the island is a generic feature related directly to the degree of development of the horseshoe as measured by the formal parameter  $\alpha$  [8]. The period of rotation  $T$  at the surface is given by

$$T = n + 3/2 \quad \text{if} \quad \alpha \propto 2^{-n}, \quad (9)$$

with  $n$  integer. The derivation of this result will be presented elsewhere [11]. For  $A = 0.967$  we have  $T \approx 10.5$  and thus the period of rotation we see (Fig. 3), is smaller than this estimate. This shortening of period is not surprising and confirms that we really see a tunneling into the stable island. As we expect, the winding time decreases as we approach the center of the island, (see Fig. 1).

We evaluate the total intensity inside the potential well as a function of time  $I_w(t)$ . In Fig. 4

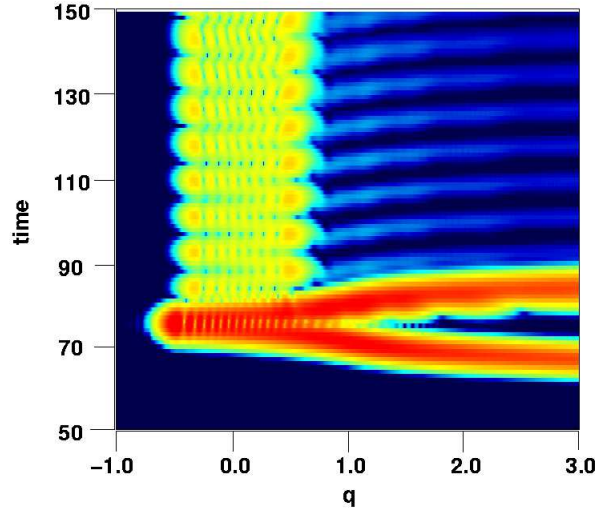


Fig. 3 – Probability distribution in configuration space as a function of time in a logarithmic colour-scale. After most of the probability has been scattered, a part stays in the potential well trapped by the stable island. This decays exponentially in echoes with a period  $T \approx 8.6$  with an estimated error of 5%. Parameters and initial conditions are as in Fig. 2.

we see that the decay is oscillatory (inset), with near constant period, but with exponentially diminishing envelope.

We may suspect that the echoes we see are a pure quantum phenomenon, because of the

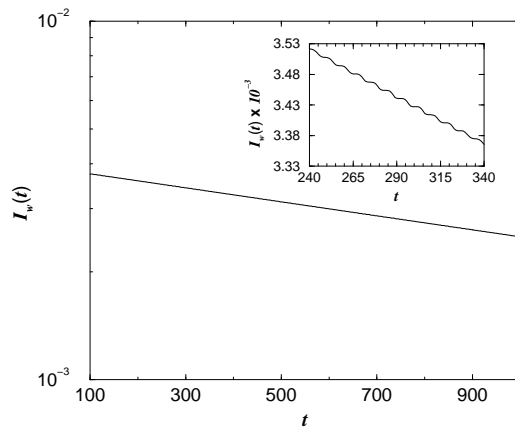


Fig. 4 – Semi-logarithmic plot of the total intensity inside the potential well as a function of time,  $I_w(t)$ . The incoming wave packet is set as in Fig. 2. In the inset, a zoom of  $I_w(t)$  is shown in linear scale where the oscillations in the decay are clearly visible.

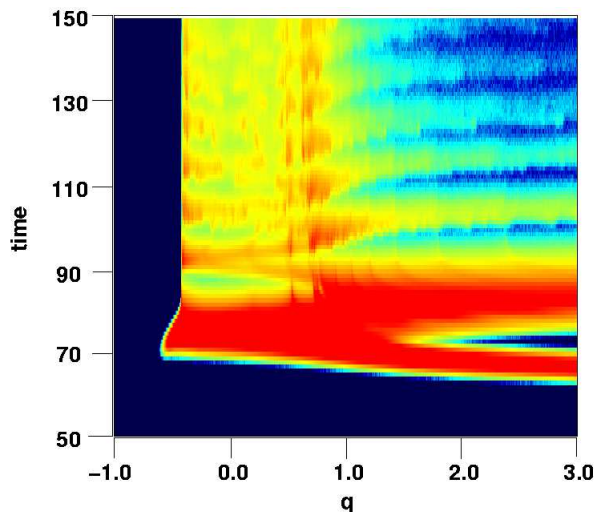


Fig. 5 – Density distribution of classical scattered orbits as a function of time in a logarithmic colour-scale, for  $A = 0.967$ . The initial conditions of the classical orbits are so, that the incoming classical packet resembles the quantum Husimi function in phase space. The period of the echoes is  $\approx 10.9$  but the error is much larger than in the quantum case.

tunneling displayed by the wave packets. Interestingly this is not entirely true. The whole sticky fractal structure of ever smaller islands rotates with the outer invariant surfaces of the main island. Therefore, a small fraction of the intensity of a packet of classically scattered particles will have a similar behaviour, though three differences are notable: First the period is equal to the one predicted at the surface and therefore, larger than the quantum period, second the wave packet spreads more rapidly and third the decay beyond the oscillations is governed by a power-law; the staying probability decays with a power of roughly  $2.554 \pm 0.005$  as is expected for a mixed phase space [12, 13]. In Fig. 5 we plot the intensity of a packet of scattered classical particles. Note that the amplitude of the oscillation clearly indicates that it takes place in the sticky region.

Returning to quantum mechanics we can also use long pulses with high energy resolution to analyze the same phenomenon in the energy domain. In Fig. 6 we plot the total intensity remaining in the potential well at time  $t = 450$  as a function of the incoming energy for a strength parameter  $A = 2$ . We clearly see the two periods characteristic of our problem, namely the period of the pulsed system and the one corresponding to the echoes which now is shorter as the island is smaller. We also calculated the  $S$ -matrix as a function of the quasienergy. It shows the same resonances we see in Fig. 6 but, a good resolution is harder to obtain. The presence of these sharp resonances is an additional indication that tunneling between the regular and chaotic regions of the classical phase portrait occurs [14].

We have proposed the possibility to explore scattering systems corresponding to binary and other low order horseshoes with wave and classical scattering experiments, and find characteristic phenomena, which we call echoes, if we use short pulses as input. From a theoretical point of view it is interesting that experiments performed along these lines are sensitive to the degree of development of the corresponding horseshoe, giving us a powerful tool to explore low developed horseshoes, where it is very hard, if not impossible, to obtain the symbolic dynamics as pruning sets in at a very low level [3].

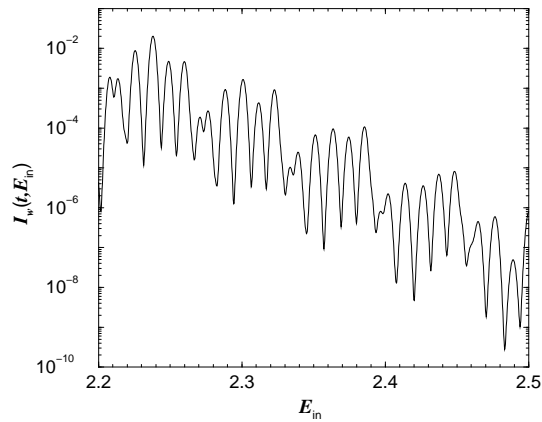


Fig. 6 – Semi-logarithmic plot of the total intensity remaining in the potential well at time  $t = 450$  as a function of the incoming energy. This is calculated for a long pulse with  $\sigma = 10$ ,  $A = 2$  and  $\hbar = 0.01$ .

From a practical point of view experiments with similar time dependent Hamiltonians are feasible in scattering of atoms on surfaces [5] in the classical or almost classical domain, whereas the corresponding experiments with electromagnetic waves seem quite feasible with ternary horseshoes generated in appropriate cavities [6]. Similar experiments can be performed on mesoscopic scale.

We acknowledge useful discussions with F. Leyvraz, P. Seba and H.-J. Stöckmann. Financial support by DGAPA-UNAM, project IN109000 and by CONACyT, project 25-192-E is acknowledged. C.M. acknowledges a fellowship by DGEP-UNAM.

## REFERENCES

- [1] SMALE S., *Bull. Am. Math. Soc.*, **73** (1967) 747.
- [2] JUNG C., LIPP C. and SELIGMAN T. H., *Ann. Phys. (N.Y.)*, **275** (1999) 151.
- [3] RÜCKERL B. and JUNG C., *J. Phys. A: Math. Gen.*, **27** (1994) 55.
- [4] BORONDO F., ZEMBEKOV A. A. and BENITO R. M., *J. Chem. Phys.*, **105** (1996) 5068.
- [5] RAIZEN M., (private communication).
- [6] RICHTER A., (private communication).
- [7] BURGHARDT I. and GASPARD P., *J. Chem. Phys.*, **100** (1994) 6395.
- [8] MEJIA-MONASTERIO C., *PhD Thesis, University of Mexico (UNAM) 2001*
- [9] DAVIS M. J., MACKAY R. S. and SANNAMI A., *Physica D*, **52** (1991) 171.
- [10] TROLL G., *Chaos*, **3** (1993) 459.
- [11] JUNG C., MEJIA-MONASTERIO C. and SELIGMAN T. H., to be published.
- [12] KARNEY C. F., *Physica D*, **8** (1983) 360.
- [13] CHIRIKOV B. and SHEPELYANSKY D. L., *Physica D*, **13** (1984) 395.
- [14] SEBA P., *Phys. Rev. E*, **47** (1993) 3870